JACS
JOURNAL OF THE AMERICAN CHEMICAL SOCIETY
Communication
pubs.acs.org/JACS

Patterned Monolayer Self-Assembly Programmed by Side Chain Shape: Four-Component Gratings

Yi Xue and Matthew B. Zimmt*

Department of Chemistry, Brown University, Providence, Rhode Island 02912, United States

Supporting Information

ABSTRACT: A molecular recognition strategy based on alkadiyne side chain shape is used to self-assemble a four-component, 1D-patterned monolayer at the solution–HOPG interface. The designed monolayer unit cell contains six molecules and spans 23 nm × 1 nm. The unit cell's internal structure and packing are driven by complementary shapes and lengths of six different alkadiyne side chains. A solution of the four compounds on HOPG self-assembles monolayers (i) comprised, almost entirely, of the intended unit cell, (ii) exhibiting patterned domains spanning 10^4 nm^2, and (iii) which are sufficiently robust that patterned domains survive solvent rinsing and drying. The patterned monolayer affords 1D-feature spacings ranging from 3.3 to 23 nm. The results demonstrate the remarkable selectivity afforded by molecular recognition based on alkadiyne side chain shape and the ability to program highly complex 1D-patterns in self-assembled monolayers.

Self-assembled monolayers with designed supramolecular structure continue to be of great interest.[1] Such compositionally patterned monolayers have potential as templates to direct multilayer assembly[2] or as tools to probe nm-length scale phenomena in chemistry, biology, and physics. While there are many examples of two-[3] and three-component[4] monolayers, few of these exhibit supramolecular features spanning 10 nm or more.[3e,f] Tailoring the monolayer structure on these length scales requires bigger molecules[5] and/or larger sets of molecular components that scrupulously select neighboring molecules in the monolayer. As examples of four-component self-assembled monolayers are rare,[6] development of robust strategies for engineering supramolecular structure in multicomponent monolayers remains an important and unsolved challenge. Here we demonstrate the potency of molecular shape selection[7] by alkadiyne side chains to program supramolecular structure in multicomponent monolayers; the designed four-component monolayer exhibits supramolecular structure (i) assembled, almost exclusively, from one out of more than 6 × 10^4 possible, six-molecule building blocks, (ii) built on a 1D-pattern repeat that spans 23 nm, and (iii) that retains pattern registration for hundreds of nanometers. The monolayer survives solvent rinsing and drying and exhibits uninterrupted supramolecular structure across areas as large as 10^4 nm^2.

Supramolecular assembly requires molecular recognition among components.[8] Molecular recognition based on coordinate covalent[9] or hydrogen bonding[10] has been used to direct monolayer self-assembly. The geometric constraints of a planar substrate and monolayer prompted this effort to use aliphatic side chains with "Tetris-like" shapes (Chart 1) to realize molecular recognition and supramolecular assembly in monolayers formed from mixtures of 1,5-(side chain)-substituted anthracenes. Optimized van der Waals interactions from close packing of specific pairs of shape complementary side chains is the anticipated energetic basis for molecular recognition.[11] Monolayers assembled by these substituted anthracene derivatives exhibit alternating aryl and aliphatic columns. The aliphatic columns contain interdigitated side chains attached, alternately, to anthracenes in the flanking aryl columns. This morphology promotes assembly of adjacent anthracene columns bearing identical length side chains; i.e. the aliphatic columns segregate side chains by length.[3f,12] However, length alone cannot differentiate multiple molecules bearing the same length side chain.[12] Additional structural differences and interactions are needed to implement such selection. This study uses the kinked shape of alka-*n*,*n*+2-diynes to select among identical length chains. Each internal diyne group creates a 0.3 nm offset between two parallel, terminal alkyl groups. Diyne "kinks" located near the aryl core or near the chain terminus reduce van der Waals contacts between *identical*, interdigitated

Chart 1. Self-Incommensurate (top) and Pairwise Complementary (bottom) Alka-*n*,*n*+2-diyne Side Chains[a]

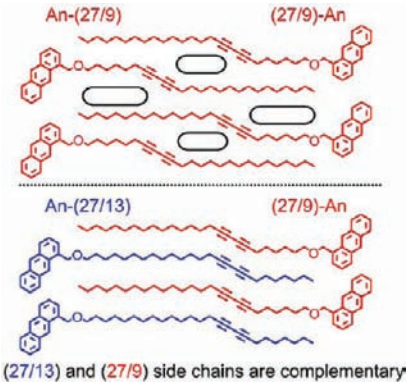

[a]Side chains are characterized (*X*/*Y*) by length (*X* = number of C + O atoms) and the side chain position (*Y*) of the first alkyne carbon. Black ovals indicate regions lacking chain–chain van der Waals contact.

Received: December 19, 2011
Published: February 28, 2012

   dx.doi.org/10.1021/ja2115019 | *J. Am. Chem. Soc.* 2012, 134, 4513–4516

Chart 2. Structures, Intended Neighbor Selection, and Half the Designed Unit Cell of Diyne Bearing Anthracenes[a]

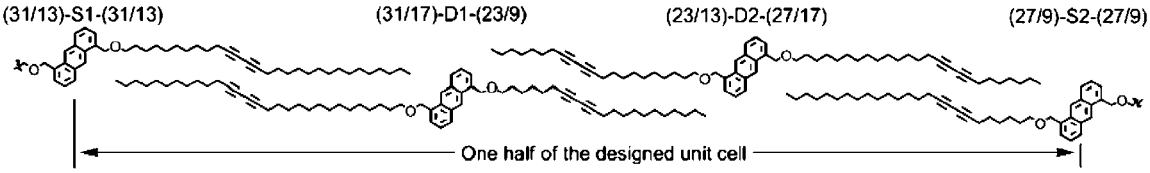

[a]Side chains are characterized (X/Y) by length (X = the number of non-hydrogen atoms) and the side chain position (Y) of the first alkyne carbon.

side chains (Chart 1, top); the chains are shape "self-incommensurate". By contrast, interdigitation of side chains with complementary kink locations yields optimal contacts and van der Waals stabilization (Chart 1, bottom). Pairwise "*shape* complementarity" affords molecular recognition and selection from among identical *length* diyne side chains.[13]

In this study, four anthracenes bearing a total of six different diyne side chains were prepared and their self-assembly on graphite was studied.[14a] Side chain shape was modulated using both chain length (23, 27, and 31 heavy atoms) and diyne "kink" location to produce two "self-incommensurate", but pair wise complementary, diyne side chains of each length. A unit cell comprised of six molecules was designed to contain one copy of two molecules with C_{2h} symmetry (**S1** and **S2**) and two copies of two molecules with C_h symmetry (**D1** and **D2**). Chart 2 displays the intended, shape-based neighbor selection of the four molecules and half the designed, C_{2h} symmetric unit cell. With six side chains and two enantiotopic faces per molecule,[15] >6 × 10^4 enantiomeric pairs of six-molecule units[14b] might assemble on HOPG, but the designed unit cell dominates.

Figure 1 displays a monolayer section self-assembled on HOPG from a phenyloctane solution of the four compounds (0.4 mM **S1**, **S2**; 0.8 mM **D1**, **D2**). The anthracene cores appear as 3 × 2 dot, high-tunneling patterns (yellow) and assemble as columns via close approach of adjacent anthracenes' corners. The long axes of all anthracenes are parallel (horizontal in Figure 1), indicating adsorption to HOPG via the same enantiotopic face. The center to center spacings of the four anthracene columns crossing the green rectangle in Figure 1 are 3.8, 3.3, and 4.4 nm. These distances are in good agreement with anthracene column spacings obtained from a monolayer simulation on graphene (Table 1):

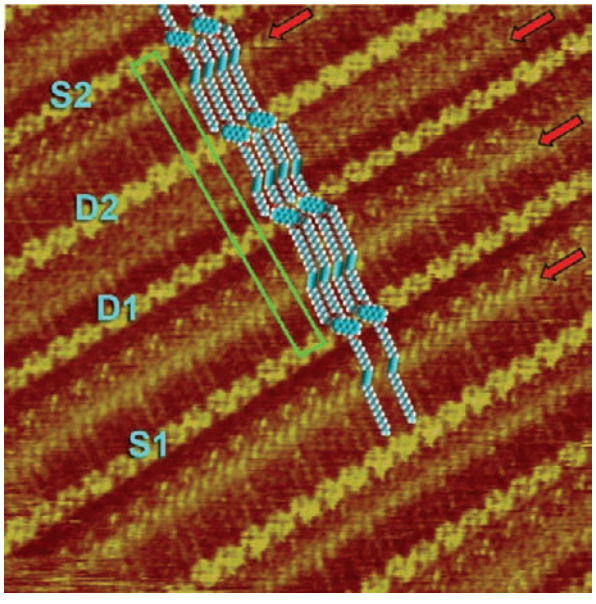

Figure 1. Constant current image (0.85 V, 0.1 nA, 20 nm × 20 nm) of the monolayer assembled from a phenyloctane solution of **S1**, **D1**, **D2**, and **S2**. Red arrows mark diyne columns. The asymmetric unit (green rectangle) parameters are a = 11.5 ± 0.4 nm, b = 0.93 ± 0.05 nm, α = 91 ± 3°.

Table 1. Measured and Simulated Spacings (nm) of Nearest Anthracene and Diyne Columns[14c]

Molecule	S2		D2		D1		S1
	AnCOC$_6$-cccc-C$_{15}$		C$_{11}$-cccc-C$_6$OCAnCOC$_{14}$-cccc-C$_{11}$				
			C$_7$-cccc-C$_{14}$OCAnCOC$_{10}$-cccc-C$_7$		C$_{15}$-cccc-C$_{10}$OCAn		
Measured	1.5	2.4	1.8	1.5	2.4	2.0	
Simulated	1.50	2.42	1.86	1.49	2.47	2.01	

3.92 nm for **S2**-**D2**, 3.35 nm for **D2**-**D1**, and 4.48 nm for **D1**-**S1**.[14c] Diffuse, lower-tunneling diyne columns (red arrows, Figure 1) run parallel to the anthracene columns. The close packing and linearity of the diyne columns, along with the measured anthracene−diyne spacings (Table 1), is consistent with the shape based molecular recognition proposed in Chart 2 and confirms the anthracene column compositions as **S2**, **D2**, **D1**, and **S1** from top to bottom along the unit cell asymmetric unit (green rectangle).

The complete unit cell of the 1D patterned monolayer is visible in larger monolayer sections (Figure 2). At this length scale, the anthracene columns are visible, but the anthracene 3 × 2 dot patterns are not. The stacked diyne column edges exhibit STM contrast, appearing as "train tracks" within the aliphatic columns (red arrows). Once again, the anthracene and diyne spacings identify the column compositions and confirm the 1D patterned monolayer unit cell contains six molecules in the order **S1**-**D1**-**D2**-**S2**-**D2**-**D1**. The image in Figure 2 was recorded at the air−HOPG interface. After a 3 μL drop of the phenyloctane solution was applied to HOPG and annealed at 40 °C for 2 h, the sample was rinsed with 2 mL of cold ethanol to remove the phenyloctane solution and then air-dried for 1 h. Figure 2 demonstrates that monolayer physisorption to the HOPG is sufficient to resist the forces active during solvent washing and drying.[16] A defect near the bottom of the left **D2** column consists of two **D2** molecules with improperly directed side chains.[14d] This defect was absent from the next STM scan.[14d]

A 140 nm × 140 nm STM scan of a similarly prepared "dry" sample characterizes the spatial persistence of the monolayer pattern (Figure 3). Diyne column locations are not discernible at this image scale, so the sequence of anthracene column spacings serves to identify column compositions. In the direction perpendicular to the anthracene columns (red line), the designed anthracene spacing pattern persists for at least 160 nm (>7 unit cells). In the direction parallel to the anthracene

dx.doi.org/10.1021/ja2115019 | J. Am. Chem. Soc. 2012, 134, 4513−4516

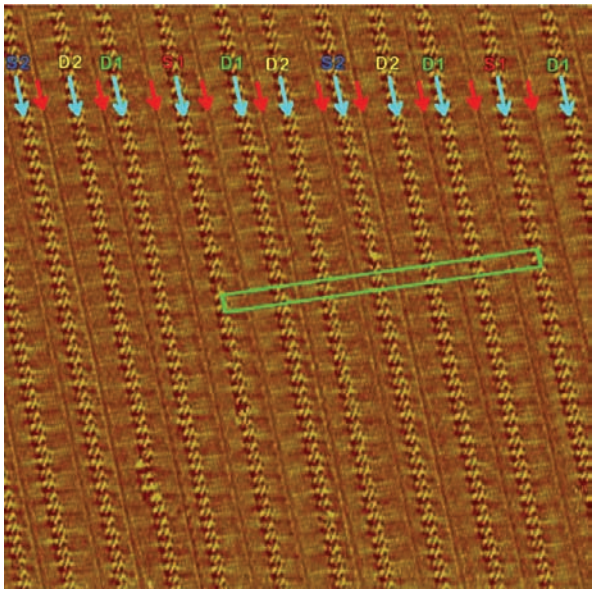

Figure 2. Constant height STM image (0.85 V, 0.04 nA, 43 nm × 43 nm) of the monolayer assembled from a solution of **S1**, **D1**, **D2**, and **S2**. This image was recorded at the air-HOPG interface after ethanol rinsing. Cyan (red) arrows mark anthracene (diyne) columns. The unit cell (green rectangle) parameters are a = 23.0 ± 0.9 nm, b = 0.95 ± 0.06 nm, α = 90 ± 5°. The anthracene column spacings are ~3.8 nm for **S2**/**D2**, ~3.3 nm for **D1**/**D2**, and ~4.4 nm for **D1**/**S1**.

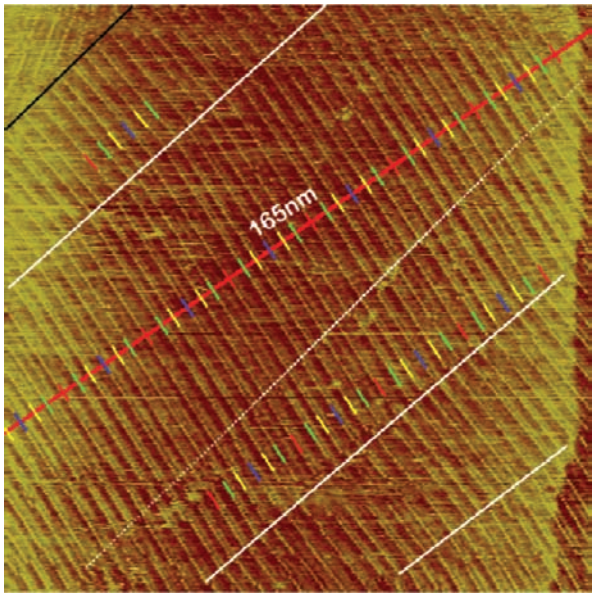

Figure 3. Constant current image (0.85 V, 0.040 nA, 140 nm × 140 nm) of the monolayer assembled from a solution of **S1**, **D1**, **D2**, and **S2**. This image was recorded at the air−HOPG interface after ethanol rinsing and drying. The long red line spans 165 nm. Solid white lines separate enantiomeric domains. The colored bars mark columns of **S1** (red), **D1** (green), **D2** (yellow), and **S2** (blue).

columns, the pattern's persistence length is shortened by various defects including (i) interfaces between enantiomeric domains[14e,15] (solid white lines), (ii) interfaces between domains related by graphite's 3-fold symmetry (black line), and (iii) single and clusters of improperly aligned/adsorbed molecules. A domain in the center of Figure 3 (between the upper solid white and dashed white lines) contains more than 2000 molecules that assemble and pack using the intended shape-based selection.

The sequence of column spacings in the region below the dashed white line confirms assembly of the intended monolayer pattern. However, the registration of the unit cells below the dashed line is shifted left by ~7.5 nm relative to the unit cells above the dashed line. Upon close inspection,[14f] anthracene columns assigned as **D2** (yellow bar) or **S1** (red bar) exhibit unbroken lines of dots (anthracenes) crossing the dashed line. By contrast, columns assigned as **D1** (green bar) or **S2** (blue bar) exhibit broken lines of dots (anthracene) in crossing the dashed white line. As the unit cells on opposite sides of the dashed line are out of registration, by two columns, every column must contain at least one defect, i.e., a change in orientation or identity of adjacent anthracenes. The packing of these defects must be characterized and understood in order to increase pattern persistence parallel to the anthracene columns.

The presence of all four compounds is *sufficient* to direct self-assembly of patterned monolayers, but is it *necessary*? For this control and to check the fidelity of side chain molecular recognition, phenyloctane solutions lacking one of the four compounds were applied to HOPG.[14g] No STM detectable monolayers are observed when **S1**, **D1**, or **D2** is excluded from solutions of the other three compounds. The three molecules in each of these solutions are not adequate to substitute for the missing compound and assemble a monolayer. Exclusion of **S2** from the mixture of compounds did produce monolayers comprised of small domains (<35 nm in both directions) exhibiting various spacing patterns between anthracene columns.[14g] The most common of these column spacing patterns, a (4.4 nm-3.3 nm-4.4 nm)$_X$ repeat, can be rationalized as substitution of **S1** for the missing **S2**; i.e. (**S1**-**D1**-**D2**)$_X$. The 31 atom side chain of **S1** can pack its diyne carbons and outer 15 CH_2 units in registration with the diyne carbons and inner 16 CH_2/O units of **D2**.[14h] Although **S1** can fill in for the absence of **S2** in three-component monolayers, the lack of any (4.4 nm-3.3 nm-4.4 nm)$_X$ repeat in monolayers formed from all four compounds suggests greater stability (selectivity) of the **D2**-**S2** contact compared to the **D2**-**S1** contact. Although the **S1**, **D1**, **D2** mixture does assemble monolayers, the domains' limited spatial extents and frequent 1D pattern disruption indicate reduced stability and robustness compared to the large domains and pattern coherence in the monolayer assembled by all four components.

In conclusion, the self-assembly of complex, supramolecular structure in monolayers can be programmed using shape complementarity of alkadiyne side chains. The four molecular shapes used here afford excellent, albeit imperfect, molecular recognition. In addition, the two, long alkadiyne side chains on each molecule and the assembly of dense-packed domains produce robustly physisorbed monolayers that survive solvent rinsing and drying. This strategy for side chain shape based patterning of monolayers should be scalable to unit cells of sufficient length (~50 nm) that a single repeat can be interfaced with top-down assembly tools.[17] Efforts to improve molecular recognition fidelity, to increase unit cell size and complexity, and to use monolayers as templates are ongoing.

■ ASSOCIATED CONTENT

Ⓢ Supporting Information

Syntheses and spectral data, STM sample preparation and acquisition procedures, adsorption orientations and estimated count of unique unit cells, STM images of three-component

dx.doi.org/10.1021/ja2115019 | J. Am. Chem. Soc. 2012, 134, 4513−4516

monolayers, Figure 3 zoomed views, molecular mechanics simulation and chain energetics, defect models. This material is available free of charge via the Internet at http://pubs.acs.org.

AUTHOR INFORMATION

Corresponding Author

mbz@brown.edu

Notes

The authors declare no competing financial interest.

ACKNOWLEDGMENTS

We gratefully acknowledge computational assistance from Dr. Wenjun Tong, data collection assistance from Tereza Pašková, and financial support from the National Science Foundation (CHE1058241).

REFERENCES

(1) (a) Elemans, J. A. A. W.; Lei, S.; De Feyter, S. *Angew. Chem., Int. Ed.* **2009**, *48*, 7298−7232. (b) Hermann, B. A.; Scherer, L. J.; Housecroft, C. E.; Constable, E. C. *Adv. Funct. Mater.* **2006**, *16*, 221−235. (c) Lackinger, M.; Heckl, W. M. *Langmuir* **2009**, 11307−11321.

(2) (a) Theobald, J. A.; Oxtoby, N. S.; Phillips, M. A.; Champness, N. R.; Beton, P. H. *Nature* **2003**, *424*, 1029−1031. (b) Wei, Y.; Reutt-Robey, J. E. *J. Am. Chem. Soc.* **2011**, *133*, 15232−15235. (c) Blunt, M. O.; Russell, J. C.; Gimenez-Lopez, M. C.; Taleb, N.; Lin, X.; Schröder, M.; Champness, N. R.; Beton, P. H. *Nat. Chem.* **2011**, *3*, 74−78. (d) Bléger, D.; Mathevet, F.; Kreher, D.; Attias, A.-J.; Bocheux, A.; Latil, S. L.; Douillard, L.; Fiorini-Debuisschert, C.; Charra, F. *Angew. Chem., Int. Ed.* **2011**, *50*, 6562−6566.

(3) (a) Eichhorst-Gerner, K.; Stabel, A.; Moessner, G.; Declerq, D.; Valiyaveettil, S.; Enkelmann, V.; Müllen, K.; Rabe, J. P. *Angew. Chem., Int. Ed.* **1996**, *35*, 1492−1495. (b) Vanoppen, P.; Grim, P. C. M.; Rücker, M.; De Feyter, S.; Moessner, G.; Valiyaveettil, S.; Müllen, K.; De Schryver, F. C. *J. Phys. Chem.* **1996**, *100*, 19636−19641. (c) Qian, P.; Nanjo, H.; Yokoyama, T.; Suzuki, T. M. *Chem. Commun.* **1999**, 1197−1198. (d) Hipps, K. W.; Scudiero, L.; Barlow, D. E.; P. Cooke, M. P. *J. Am. Chem. Soc.* **2002**, *124*, 2126−2127. (e) Plass, K. E.; Engle, K. M.; Cychosz, K. A.; Matzger, A. J. *Nano Lett.* **2006**, *6*, 1178−1183. (f) Wei, Y.; Tong, W.; Zimmt, M. B. *J. Am. Chem. Soc.* **2008**, *130*, 3399−3405. (g) Treier, M.; Nguyen, M.-T.; Richardson, N. V.; Pignedoli, C.; Passerone, D.; Fasel, R. *Nano Lett.* **2009**, *9*, 126−131. (h) Palma, C.-A.; Bjork, J.; Bonini, M.; Dyer, M. S.; Llanes-Pallas, A.; Bonifazi, D.; Persson, M.; Samorì, P. *J. Am. Chem. Soc.* **2009**, *131*, 13062−13071. (i) Schmaltz, B.; Rouhanipour, A.; Räder, H. J.; Pisula, W.; Müllen, K. *Angew. Chem., Int. Ed.* **2009**, *48*, 720−724. (j) Wintjes, N.; Lobo-Checa, J.; Hornung, J.; Samuely, T.; Diederich, F.; Jung, T. A. *J. Am. Chem. Soc.* **2010**, *132*, 7306−7311. (k) Zhang, X.; Chen, T.; Yan, H.-J.; Wang, D.; Fan, Q.-H.; Wan, L.-J.; Ghosh, K.; Yang, H.-B.; Stang, P. J. *ACS Nano* **2010**, *4*, 5685−5692. (l) Liang, H.; Sun, W.; Jin, X.; Li, H.; Li, J.; Hu, X.; Teo, B.; Wu, K. *Angew. Chem., Int. Ed.* **2011**, *50*, 7562−7566.

(4) (a) Llanes-Pallas, A.; Matena, M.; Jung, T.; Prato, M.; Stöhr, M.; Bonifazi, D. *Angew. Chem., Int. Ed.* **2008**, *47*, 7726−7730. (b) Lei, S.; Surin, M.; Tahara, K.; Adisoejoso, J.; Lazzaroni, R.; Tobe, Y.; De Feyter, S. *Nano Lett.* **2008**, *8*, 2541−2546. (c) Silly, F.; Shaw, A. Q.; Porfyrakis, K.; Warner, J. H.; Watt, A. A. R.; Castell, M. R.; Umemoto, H.; Akachi, T.; Shinoharad, H.; Briggs, G. A. D. *Chem. Commun.* **2008**, 4616−4618.

(5) Segalman, R. A. *Mater. Sci. Eng. R* **2005**, *48*, 191−226.

(6) (a) Adisoejoso, J.; Tahara, K.; Okuhata, S.; Lei, S.; Tobe, Y.; De Feyter, S. *Angew. Chem., Int. Ed.* **2009**, *48*, 7353−7357. (b) Le, J. D.; Pinto, Y.; Seeman, N. C.; Musier-Forsyth, K.; Taton, T. A.; Kiehl, R. A. *Nano Lett.* **2004**, *4*, 2343−2347.

(7) (a) Mali, K. S.; Averbeke, B. V.; Bhinde, T.; Brewer, A. Y.; Arnold, T.; Lazzaroni, R.; Clarke, S. M.; De Feyter, S. *ACS Nano* **2011**, *5*, 9122−9137. (b) Shao, X.; Luo, X.; Hu, X.; Wu, K. *J. Phys. Chem. B* **2006**, *110*, 15393−15402.

(8) Lehn, J.-M. *Science* **1993**, *260*, 1762−1763.

(9) (a) Semenov, A.; Spatz, J. P.; Moller, M.; Lehn, J. M.; Sell, B.; Schubert, D.; Weidl, C. H.; Schubert, U. S. *Angew. Chem., Int. Ed.* **1999**, *38*, 2547−2550. (b) Li, S.-S.; Northrop, B. H.; Yuan, Q.-H.; Wan, L.-J.; Stang, P. J. *Acc. Chem. Res.* **2009**, *42*, 249−259.

(10) (a) Dienstmaier, J. F.; Mahata, K.; Walch, H.; Heckl, W. M.; Schmittel, M.; Lackinger, M. *Langmuir* **2010**, *26*, 10708−10716. (b) Ivasenko, O.; Perepichka, D F. *Chem. Soc. Rev.* **2011**, *40*, 191−206.

(11) (a) Dickerson, P. N.; Hibberd, A. M.; Oncel, N.; Bernasek, S. L. *Langmuir* **2010**, *26*, 18155−18161. (b) Piot, L.; Marchenko, A.; Wu, J.; Müllen, K.; Fichou, D. *J. Am. Chem. Soc.* **2005**, *127*, 16245−16250. (c) Tahara, K.; Johnson, C. A. II; Fujita, T.; Sonoda, M.; De Schryver, F. C.; De Feyter, S.; Haley, M. M.; Tobe, Y. *Langmuir* **2007**, *23*, 10190−10197.

(12) Yablon, D. G.; Ertas, D.; Fang, H.; Flynn, G. W. *Isr. J. Chem.* **2003**, *43*, 383−392.

(13) Xue, Y.; Zimmt, M. B. *Chem. Commun.* **2011**, *47*, 8832−8834.

(14) See the Supporting Information for (a) compound and monolayer, preparations, and characterization, (b) the 12 possible adsorption orientations and estimate of the number of unique unit cells, (c) a molecular mechanics minimized monolayer section (CPK models) and key spacings, (d) a model of the **D2** defect (in Fig. 2) and the next STM scan, (e) an STM image of the interface between enantiomeric domains, (f) a magnified image centered around the dashed white line in Figure 3, (g) conditions and STM images of the three-component control experiments, and (h) a model of the (**S1**-**D1**-**D2**)$_X$ three-component repeat and molecular mechanics energy estimates of various side chain (and defect) packings.

(15) (a) Elemans, J. A. A. W.; De Cat, I.; Xu, H.; De Feyter, S. *Chem. Soc. Rev.* **2009**, *38*, 722−736. (b) Katsonis, N.; Lacaze, E.; Feringa, B. L. *J. Mater. Chem.* **2008**, *18*, 2065−2073. (c) Wei, Y.; Kannappan, K.; Flynn, G. W.; Zimmt, M. B. *J. Am. Chem. Soc.* **2004**, *126*, 5318−5322. (d) Tong, W.; Wei, X.; Zimmt, M. B. *J. Phys. Chem. C* **2009**, *113*, 17104−17113.

(16) (a) Byun, M.; Han, W.; Qiu, F.; Bowden, N. B.; Lin, Z. *Small* **2010**, *6*, 2250−2255. (b) Lee, S. L.; Chi, C. Y.; Huang, M. J.; Chen, C. H.; Li, C. W.; Pati, K.; Liu, R. S. *J. Am. Chem. Soc.* **2008**, *130*, 10454−10455. (c) Prevo, B. G.; Velev, O. D. *Langmuir* **2004**, *20*, 2099−2107.

(17) Madueno, R.; Räisänen, M. T.; Silien, C.; Buck, M. *Nature* **2008**, *454*, 618−621.